CHEMICAL ENGINEERING TRANSACTIONS
VOL. 94, 2022
A publication of AIDIC
The Italian Association of Chemical Engineering
Online at www.cetjournal.it
Guest Editors: Petar S. Varbanov, Yee Van Fan, Jiří J. Klemeš, Sandro Nižetić

ISBN 978-88-95608-93-8; **ISSN** 2283-9216
DOI: 10.3303/CET2294108

Effect of porosity on the Performance of PCHE with Embedded PCM/EG under Fluctuating Temperature Conditions

Lianjie Zhang[a], Jiří Jaromír Klemeš[b], Xinyi Luo[a], Min Zeng[a,*], Qiuwang Wang[a]

[a] Key Laboratory of Thermo-Fluid Science and Engineering, MOE, School of Energy and Power Engineering, Xi'an Jiaotong University, Xi'an, Shanxi, 710049, P.R. China.
[b] Sustainable Process Integration Laboratory – SPIL, NETME Centre, Faculty of Mechanical Engineering, Brno University of Technology – VUT Brno, Technická 2896/2, 616 69 Brno, Czech Republic
zengmin@mail.xjtu.edu.cn

The supercritical CO2 Brayton cycle is widely utilized by various industries because of its compactness and efficiency. However, in the actual process, there are always temperature fluctuations that affect the normal operation of the whole supercritical CO2 Brayton cycle system, in order to weaken the temperature fluctuations without adding additional components, a new structure of PCHE with PCM embedded in PCHE was designed in this study. Fluent was used to simulate the working conditions and compare with the commonly used PCHE under the same working conditions. It was found that the structures with porosity of 0.8 to 0.9, the percentage reduction of temperature fluctuations on the hot side was 26.84 %, 26.78 % and 26.49 %, respectively, and the percentage reduction of temperature fluctuations on the cold side was 40.30 %, 40.81 % and 41.63 %, respectively, and the percentage reduction of heat exchange was 1.8 %, 1.9 % and 2.3 %, respectively.

1. Introduction

Heat exchanger is an essential component of supercritical CO_2(SCO_2) system (Zhang, et al.,2020), for recompression layout, low temperature heat exchanger, high temperature heat exchanger, condenser and heat absorber are all heat exchangers in essence (Xu, et al.,2019), the common structure is PCHE (because of its compactness and high efficiency), and in the actual application, the hot side inlet of high temperature heat exchanger often has large temperature fluctuations (Zhang, et al.,2021). The temperature fluctuations can usually be attenuated by suitable PCM (Peng, et al.,2021), but this introduces additional storage tanks for PCM. Therefore, the new structure of PCM directly embedded in PCHE is worth studying. Considering that the thermal conductivity of PCM is usually much lower than that of metallic materials, the composite structure of PCM and expanded graphene (Wu, et al.,2015) or metal foam (Zheng, et al.,2021) is often used to enhance the thermal conductivity of PCM. In addition, the utilization rate of PCM is also an issue of concern, because the temperature difference between the two ends of the high-temperature heat exchanger is large, so the need to use a multi-layer PCMs ladder arrangement (Sadeghi, et al.,2020) will make the same volume of PCM can be more in the phase change temperature point, the rate of higher utilization. Therefore, in this study, a new structure of PCM composite expanded graphene embedded in PCHE is designed to replace the conventional high-temperature heat exchanger in the SCO2 cycle, and the effect of the new structure on the weakening effect of temperature fluctuations and the degree of influence on the heat exchange when the hot-side temperature fluctuates is simulated using the software Fluent.

Paper Received: 27 April 2022; Revised: 10 May 2022; Accepted: 19 May 2022
Please cite this article as: Zhang L., Klemeš J.J., Luo X., Zeng M., Wang Q., 2022, Effect of porosity on the performance of PCHE with embedded PCM/EG under fluctuating temperature conditions, Chemical Engineering Transactions, 94, 649-654 DOI:10.3303/CET2294108

2. Model

2.1. Physical model

The physical model used in this study has a length, width and height of 200 mm, 100 mm and 40 mm respectively. It consists of five stacked PCM-PCHE cells, each consisting of a hot plate, a cold plate and two PCM plates, with the PCM plate between the hot and cold plates.

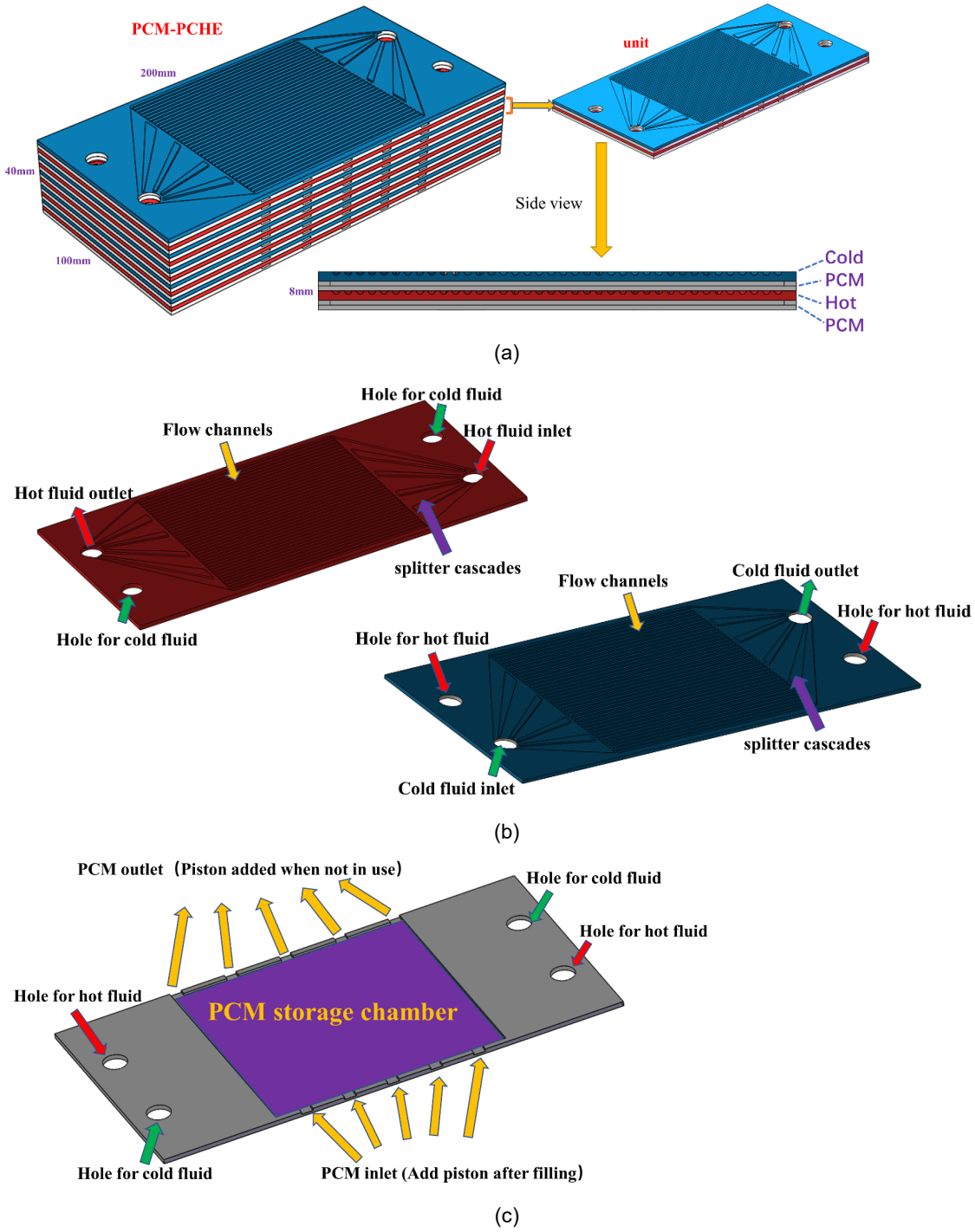

Figure. 1. Physical model diagram of PCM-PCHE: (a) Overall appearance; (b) Hot and cold plates; (c) PCM plate.

Figure 1 above shows the general appearance of the PCM-PCHE, the hot plate, the cold plate and the PCM plate respectively. Figure 1(b) shows the inlet and outlet of the hot and cold fluids in a counter-flow arrangement;

if a down-flow arrangement is required, only one fluid inlet and outlet need to be reversed. In Figure 1(c), there are five evenly spaced PCM inlets and PCM outlets, 5 mm long and 1 mm wide, on each side of the PCM plate, which are plugged with a piston when not in use. the five holes in the PCM inlets are more concentrated to facilitate PCM filling so that the PCM storage chamber can be filled more easily, while the five holes in the PCM outlets are more dispersed to facilitate PCM drainage without piling up PCM in the corners. The hot plate, cold plate and PCM plate are all 2mm thick.

2.2. Numerical model

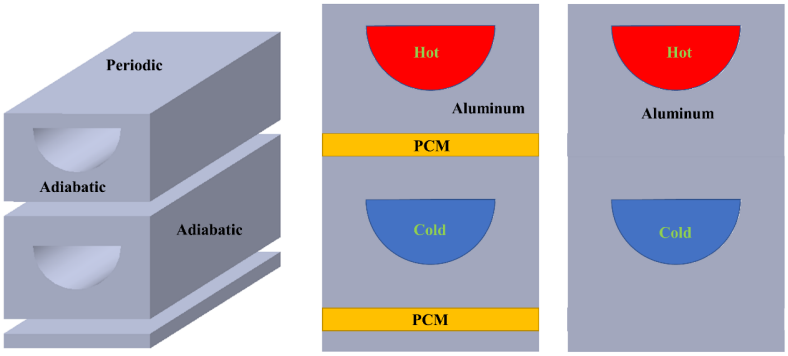

Figure 2. Schematic diagram of the cell used for simulation calculations

Figure 2 above shows the computational cell used for simulation in this paper. The cell has a length, width, and height of 100 mm, 2.5 mm, and 4 mm, respectively. Since the cell is repeated at the top and bottom, periodic boundary conditions are used for the top and bottom surfaces.

Considering the change of aluminum from the original PCHE position to PCM, the difference of thermal conductivity is large, which may have a large impact on the original heat transfer of the heat exchanger, so the situation of composite expanded graphite and PCM is used to improve the thermal conductivity of PCM and reduce the impact on the heat transfer of the heat exchanger.

The enthalpy hole model and the melting-solidification model were used to simulate the phase interface motion, solid-phase and liquid-phase heat transfer during the melting of PCM/EG in stable form. Eq (1)-Eq(3) are used to describe the flow and heat transfer characteristics of this model in the numerical study.

Energy equation:

$$\frac{\partial(\rho h_{\mathrm{p}})}{\partial t}+\nabla\cdot(\rho\vec{u}h_{\mathrm{p}})=\nabla\cdot(k\nabla T) \tag{1}$$

Momentum equation:

$$\frac{\partial(\rho\vec{u})}{\partial t}+\nabla\cdot(\rho\vec{u}\vec{u})=\mu\nabla^{2}\vec{u}-\nabla p+\rho\vec{g}+\vec{S} \tag{2}$$

Continuity equation:

$$\frac{\partial\rho}{\partial t}+\nabla\cdot(\rho\vec{u})=0 \tag{3}$$

In the equation, $\vec{u}$, $\vec{g}$, $\vec{S}$, h_{p}, T and k are velocity vector, acceleration due to gravity, the source term, total enthalpy, temperature, and thermal conductivity, where h_{p} is equal to the sum of the latent enthalpy change γL and the sensible enthalpy h_{sen} change in the phase change process, L is the latent heat, γ is the liquid fraction

$$\vec{S}=A_{musk}\frac{(1-\gamma)^{2}}{\gamma^{3}+\varepsilon}\vec{u} \tag{4}$$

Eq(4) above embodies the expression for the source term $\vec{S}$, where A_{musk} is the paste region constant, used in this study as 10^{5}. ε is a very small constant that prevents the denominator in Eq(4) from being zero, in this paper 10^{-3}.

The definition of the liquid fraction γ is as follows:

$$\gamma=0,\ \text{when}\ T<T_{\mathrm{s}};\ \gamma=1,\ \text{when}\ T>T_{\mathrm{l}};\ \gamma=\frac{T-T_{\mathrm{s}}}{T_{\mathrm{l}}-T_{\mathrm{s}}},\ \text{when}\ T_{\mathrm{s}}<T<T_{\mathrm{l}} \tag{5}$$

where T_s is the temperature at which the PCM starts to melt and T_l is the temperature at which the PCM is all melted.

To investigate the effect of the percentage of expanded graphene in the new structure of PCM/EG on the overall PCHE-PCM heat storage and heat transfer, porosity (φ) and pore density (*PPI*) are introduced, while different porosity and pore density cause changes in the viscous resistance coefficient (f_1) and inertial resistance coefficient (f_2) of PCM in the PCM/EG region.

2.3. Boundary conditions

The top and bottom of the cell used for calculations are periodic boundary conditions, the surrounding walls are adiabatic boundary conditions, and all walls within the cell are thermally coupled boundary conditions.

The velocity inlet and pressure outlet boundary conditions are used for both hot and cold fluids. The inlet velocity of the hot fluid is 4.5 m/s with an inlet temperature of 733 K. After 40 s the inlet temperature is perturbed sinusoidally with an amplitude of 25 K and a period of 16 s. The initial outlet temperature is set to 360 K. The inlet velocity of the cold fluid is 2 m/s with a constant inlet temperature of 309 K and an initial outlet temperature of 646 K. The inlet temperature on the hot side of the heat exchanger is disturbed by the temperature described in the literature.

Both hot and cold runners used carbon dioxide in the same state as in the literature, and the physical parameters in Table 1 are the constant physical conditions obtained in this study using the software REFPROP review：

Table 1 CO_2 physical properties of hot and cold runners.

	Density $(\mathrm{kg \cdot m^{-3}})$	Specific heat $(\mathrm{J \cdot kg^{-1} \cdot K^{-1}})$	Thermal conductivity $(\mathrm{W \cdot m^{-1} \cdot K^{-1}})$	Viscosity $(\mathrm{kg \cdot m^{-1} \cdot s^{-1}})$
Cold side	170.7	1252.3	0.038	2.6×10^{-5}
Hot side	77.0	1126.8	0.040	2.7×10^{-5}

3. Results and discussion

In this study, three porosities of PCM/EG were used, 0.8, 0.85, and 0.9. The thickness of the PCM layer used was 0.45 mm, and the number of PCM layers was 5.

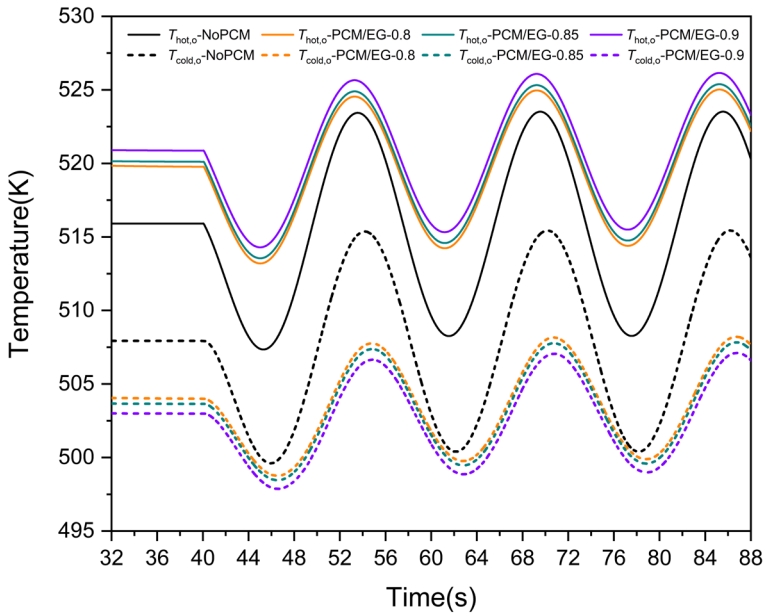

Figure 3. Comparison of outlet temperature of PCM/EG-5 with different porosity.

As shown in Figure 3 above, at 0.45 mm thickness, the amplitudes of temperature fluctuations of PCM/EG-5 cold and hot outlets with different porosities are weakened to different degrees relative to the case without PCM. Among the structures with porosity of 0.8 to 0.9, the percentage reduction of temperature fluctuations on the hot side was 26.84 %, 26.78 % and 26.49 %, respectively, and the percentage reduction of temperature fluctuations on the cold side was 40.30 %, 40.81 % and 41.63 %, respectively, and the percentage reduction of heat

exchange was 1.8 %, 1.9% and 2.3 %, respectively. It can be found that a porosity of 0.8 has a better overall effect, with a larger percentage reduction in temperature fluctuations on both the hot and cold sides and the least effect on the heat transfer rate. This is probably because smaller porosity means more graphite and less PCM, which allows more heat transfer from the hot side to the cold side and therefore has the least effect on the heat transfer.

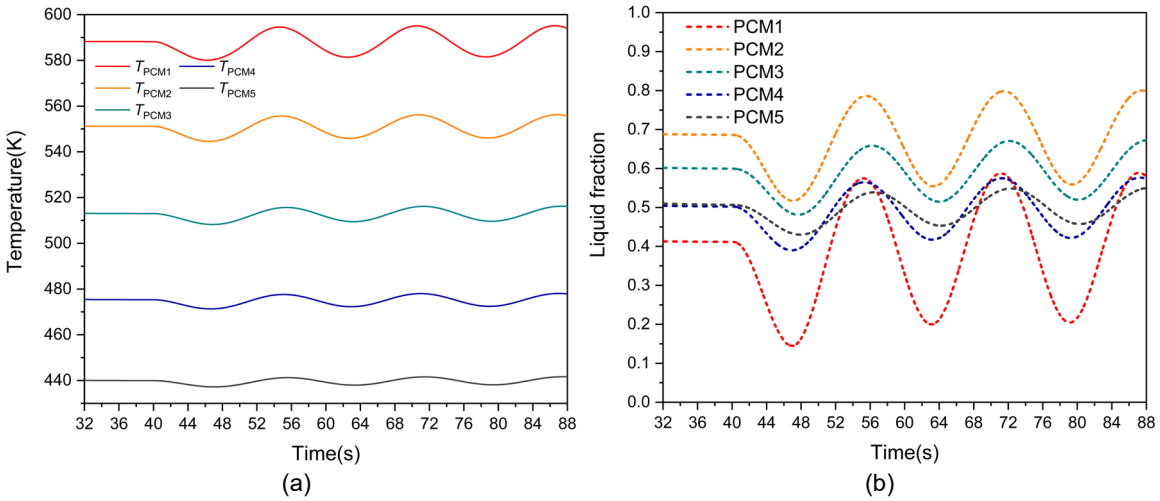

Figure 4. Five-stage PCM parameters for PCM/EG-5 with a porosity of 0.8: (a). Temperature; (b). liquid fraction.

From the above figure we can clearly see that PCM1 to PCM5 temperature and liquid phase fraction fluctuation amplitude is gradually decreasing, this is due to the process of mass flow in the channel inlet temperature fluctuations along the process is gradually weakened, the more forward PCM temperature fluctuations and liquid phase fraction fluctuations indicate a greater degree of utilization of its thermal storage characteristics, and temperature fluctuations will occur mainly because the PCM area is too flat resulting in a large temperature difference between the two ends, not all PCM are in the phase change temperature point, the two ends of the PCM is not parameter phase change so the temperature will change with the wall temperature fluctuations. In addition to this the hysteresis of temperature and liquid phase fraction fluctuations from PCM1 to PCM5 can be significantly observed.

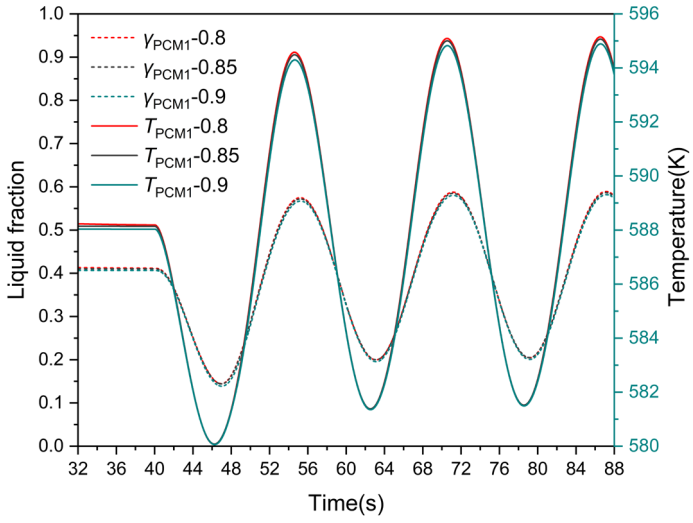

Figure 5. Fluctuations of PCM1 at different porosities.

Since PCM1 is always the piece with the largest fluctuation, Figure 5 compares the fluctuation state of PCM1 under different porosity. It can be found that when the porosity is 0.8, the fluctuation of liquid phase fraction of PCM1 is slightly larger, and the amplitude of temperature fluctuation is almost not affected by the porosity. This may be due to the fact that the total amount of PCM is less but the utilization rate is improved, and the thermal conductivity is better due to more expanded graphite.

4. Conclusions

In this study, a newly designed structure of PCM-embedded PCHE was studied parametrically, and PCM-PCHE with PCM thickness of 0.45mm was simulated using Fluent software to compare the weakening effect on temperature fluctuation and the degree of influence on heat exchange under different porosity, and the main conclusions are as follows:

(1) Among the structures with porosity of 0.8 to 0.9, the percentage reduction of temperature fluctuations on the hot side was 26.84 %, 26.78 % and 26.49 %, respectively, and the percentage reduction of temperature fluctuations on the cold side was 40.30 %, 40.81 % and 41.63 %, respectively, and the percentage reduction of heat exchange was 1.8 %, 1.9 % and 2.3 %, respectively.

(2) PCM1 to PCM5 temperature and liquid phase fraction fluctuation amplitude is gradually decreasing due to the process of mass flow in the channel inlet temperature fluctuations along the process is gradually weakened.

(3) when the porosity is 0.8, the fluctuation of liquid phase fraction of PCM1 is slightly larger, and the amplitude of temperature fluctuation is almost not affected by the porosity.

Nomenclature

A_{mush} – paste region constant, -
d_p – pore density, m^{-3}
$\vec{g}$ – acceleration due to gravity, m/s^2
h_p – total enthalpy, kJ/kg
k – thermal conductivity, W/(m·K)
L – latent heat, kJ/kg
p – pressure, Pa
Q – heat exchange, W
$\vec{S}$ – the source term, $kg/(m^2 \cdot s^2)$
T – temperature, K
τ– time, s
$\vec{u}$ – velocity vector, m/s

Greek
ε – extremely small constant, -
γ – liquid fraction, -
ΔP – pressure drop, Pa
∇ – dispersion, -
ρ – density, kg/m^3

Subscripts
MEG – Modified expanded graphene
l - liquid
NoPCM – without phase change material
PCHE – printed circuit heat exchanger
PCM – phase change material
s - solid
SCO_2 – supercritical carbon dioxide

Acknowledgments

This work has been supported by the National Key Research & Development Program of China (2018YFE0108900) and the project LTACH19033 “Transmission Enhancement and Energy Optimized Integration of Heat Exchangers in Petrochemical Industry Waste Heat Utilisation”, under the bilateral collaboration of the Czech Republic and the People’s Republic of China (partners Xi’an Jiao Tong University and Sinopec Research Institute Shanghai; SPIL VUT, Brno University of Technology and EVECO sro, Brno), programme INTER-EXCELLENCE, INTER-ACTION of the Czech Ministry of Education, Youth and Sports. Industrial & Engineering Chemistry Research.

References

Peng X., Bajaj I., Yao M., Maravelias C.T., 2021, Solid-gas thermochemical energy storage strategies for concentrating solar power:Optimization and system analysis, Energy Conversion and Management, 245, 114636.

Sadeghi H.M., Babayan M., Chamkha A., 2020, Investigation of using multi-layer PCMs in the tubular heat exchanger with periodic heat transfer boundary condition, International Journal of Heat and Mass Transfer, 147, 118970.

Wu Y., Wang T., 2015, Hydrated salts/expanded graphite composite with high thermal conductivity as a shape-stabilized phase change material for thermal energy storage, Energy Conversion and Management, 101,164-171.

Xu J., Liu C., Sun E., Xie J., Li M., Yang Y., Liu J., 2019, Perspective of S−CO2 power cycles, Energy, 186, 115831.

Zheng Z.-J., Yang C., Xu Y., Cai X., 2021, Effect of metal foam with two-dimensional porosity gradient on melting behavior in a rectangular cavity, Renewable Energy, 172, 802-815.

Zhang L., Deng T., Ma T., Zeng M., Wang Q., 2020, Selection of working medium and model for brayton cycle at different heat source temperatures, Chemical Engineering Transactions, 81, 739-744.

Zhang L., Deng T., Klemeš J.J., Zeng M., Ma T., Wang Q., 2021, Supercritical CO2 Brayton cycle at different heat source temperatures and its analysis under leakage and disturbance conditions, Energy, 237, 121610.